Photoelectron Angular Distributions as Probes of Cluster Anion Structure: I-center dot(H2O)(2) and I-center dot(CH3CN)(2)

ARTICLE *in* THE JOURNAL OF PHYSICAL CHEMISTRY A · JANUARY 2014

Impact Factor: 2.69 · DOI: 10.1021/jp4104596 · Source: PubMed

5 AUTHORS, INCLUDING:

Foster Mbaiwa
Botswana International University of Science …
17 PUBLICATIONS **99** CITATIONS
SEE PROFILE

Nicholas Holtgrewe
Howard University
9 PUBLICATIONS **11** CITATIONS
SEE PROFILE

Diep Dao
Washington University in St. Louis
5 PUBLICATIONS **13** CITATIONS
SEE PROFILE

THE JOURNAL OF PHYSICAL CHEMISTRY A

Article

pubs.acs.org/JPCA

Photoelectron Angular Distributions as Probes of Cluster Anion Structure: $I^-\cdot(H_2O)_2$ and $I^-\cdot(CH_3CN)_2$

Foster Mbaiwa,*[,†] Nicholas Holtgrewe,[‡] Diep Bich Dao,[‡] Joshua Lasinski,[‡] and Richard Mabbs*[,‡]

[†]Department of Chemistry, University of Botswana, Private Bag UB00704, Gaborone, Botswana

[‡]Department of Chemistry, Washington University in St. Louis, One Brookings Drive, St. Louis, Missouri 63130, United States

ABSTRACT: The use of photoelectron angular distributions to provide structural details of cluster environments is investigated. Photoelectron spectra and angular distributions of $I^-\cdot(H_2O)_2$ and $I^-\cdot(CH_3CN)_2$ cluster anions are recorded over a range of photon energies. The anisotropy parameter (β) for electrons undergoes a sharp change ($\Delta\beta_{max}$) at photon energies close to a detachment channel threshold. $I^-\cdot(H_2O)_2$ results show the relationship between dipole moment and $\Delta\beta_{max}$ to be similar to that observed in monosolvated I^- detachment. The $\Delta\beta_{max}$ of the 4.0 eV band in the $I^-\cdot(CH_3CN)_2$ photoelectron spectrum suggests a dipole moment of 5−6 D. This is consistent with predictions of a hydrogen bonded conformer of the $I^-\cdot(CH_3CN)_2$ cluster anion [Timerghazin, Q. K.; Nguyen, T. N.; Peslherbe, G. H. *J. Chem. Phys.* **2002**, *116*, 6867−6870].

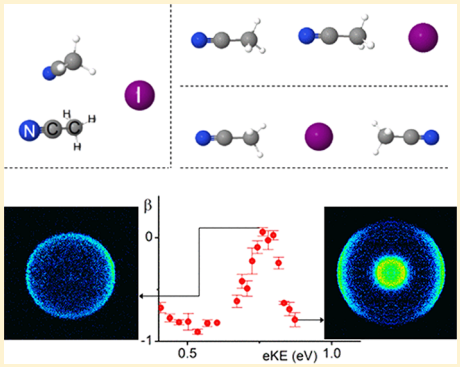

INTRODUCTION

One complication associated with studies of molecular cluster environments is the existence of several conformers—different local minima on the potential energy surface associated with a given electronic state. In this paper we highlight the possibility of using photoelectron angular distributions (PADs) as a tool to aid the assignment of spectral transitions to cluster anion conformers.

The example used will be the $I^-\cdot(CH_3CN)_2$ cluster anion, for which there have been conflicting assignments of conformers to photoelectron spectral features.[1−3] Initial work on $I^-\cdot(CH_3CN)_2$ assigned the photoelectron spectrum based on a simple electrostatic model.[2,3] Of the two bands observed in the 266 nm spectrum, the higher electron binding energy (eBE) transition was assigned to a symmetric conformer, while the lower eBE transition was attributed to a head-to-tail conformer.[2]

Later, ab initio calculations[1] suggested the possible existence of three conformers. These are shown in Figure 1, where the first two are similar to the symmetric and head-to-tail conformers of the electrostatic model. The third is stabilized by hydrogen bonding interactions. The calculated detachment energies challenged the original spectral assignments, suggesting that conformer III is responsible for the highest eBE transition, and the "symmetric" conformer (I) gives rise to the lower eBE feature. Since the conformers produced in a particular ion source are often highly dependent on the conditions employed, it was concluded that the head-to-tail conformer was not produced in the original experiment.

These spectral assignments are reassessed here, making novel use of $I^-\cdot(CH_3CN)_2$ PADs. This approach is suggested by recent studies of the electron kinetic energy (eKE) evolution of monosolvated I^- PADs in the vicinity of detachment

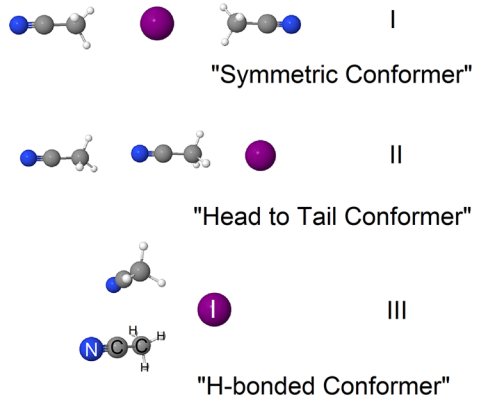

Figure 1. Three conformers of $I^-\cdot(CH_3CN)_2$ predicted by ab initio calculation.[1]

thresholds.[4−6] For a given monosolvated I^- cluster anion, two low-lying detachment channels are important. The lower eBE channel (A) produces a ground state ($^2P_{3/2}$) iodine atom, while channel B produces iodine in the lowest excited ($^2P_{1/2}$) state.

$$I^-\cdot X + h\nu \rightarrow I(^2P_{3/2}) + X + e^- \quad (A)$$

$$I^-\cdot X + h\nu \rightarrow I(^2P_{1/2}) + X + e^- \quad (B)$$

As the photon energy ($h\nu$) passes through the channel B threshold region, the PAD associated with channel A undergoes

Special Issue: Kenneth D. Jordan Festschrift

Received: October 22, 2013
Revised: January 10, 2014
Published: January 13, 2014

   dx.doi.org/10.1021/jp4104596 | *J. Phys. Chem. A* 2014, 118, 7249−7254

a rapid change. The eKE dependent anisotropy parameter (β), which characterizes the PAD, exhibits a maximum. This appears to be a common feature for monosolvated atomic halide cluster anions. Figure 2 represents similar behavior for the analogous

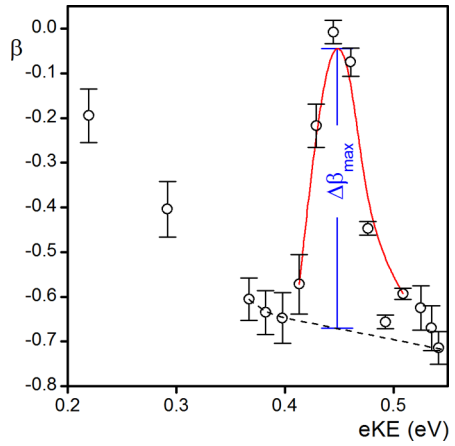

Figure 2. Variation in β with respect to eKE for channel A electrons for $Br^-{\cdot}CH_3NO_2$ detachment. Each point corresponds to a different photon energy.

channel in $Br^-{\cdot}CH_3NO_2$ detachment. By defining $\Delta\beta_{max}$ as the peak height measured from an extrapolated baseline (Figure 2, dashed line), a quantitative estimation of the strength of this effect can be made. For $I^-{\cdot}X$ cluster anions, this procedure has revealed a near linear dependence of $\Delta\beta_{max}$ on the (neutral) cluster framework dipole moment (μ) *at the equilibrium configuration of the parent anion.*[6] Therefore $\Delta\beta_{max}$ potentially represents a means of associating particular conformers with photoelectron spectral bands.

In this work we demonstrate that the $\mu-\Delta\beta_{max}$ correlation is maintained in disolvated cluster anions by using a known conformer of $I^-{\cdot}(H_2O)_2$.[7] We then apply the technique to provide further experimental evidence upon which to base assignment of photoelectron spectral features to conformers of $I^-{\cdot}(CH_3CN)_2$.

EXPERIMENTAL SECTION

Full details of the instrumentation used in this study have been provided elsewhere.[8,9] Here, only pertinent details will be included.

Photoelectron Imaging Measurements. $I^-{\cdot}(H_2O)_2$ and $I^-{\cdot}(CH_3CN)_2$ are produced in a discharge ion source.[10] CH_3I serves as a precursor for the iodine atoms upon which the cluster anions are based. A dilute CH_3I/Ar mixture (~ 5% CH_3I) at different stagnation pressures (10−80 psi) is bubbled through liquid water or acetonitrile. The mixture is expanded through a series 9 general valve pulsed nozzle operating at 10 Hz, into a vacuum chamber maintained at $\sim 10^{-5}$ Torr during operation. The pulsed discharge is applied at the throat of the expansion.

Anions are extracted into a Wiley−McLaren time-of-flight mass spectrometer.[11] Detachment from the desired anion is effected by synchronizing with the arrival time of the pulsed output of a tunable dye laser. The detachment laser is focused with a 1 m focal length spherical lens, giving average laser intensities $<1 \times 10^8$ W cm^{-2}. Measurements are taken over a range of wavelengths in the vicinity of the excited I atom channel threshold for both $I^-{\cdot}(H_2O)_2$ and $I^-{\cdot}(CH_3CN)_2$.

Detection takes place within the electrostatic lens of a photoelectron velocity map imaging arrangement,[12] with the imaging detector oriented perpendicular to ion and laser beam propagation directions. The energy resolution ($\Delta E/E$) of this perpendicular detection arrangement is approximately 0.10. The gain of the position sensitive MCP-phosphor detector is raised by application of a high voltage pulse within a 200 ns window around the instant of photoexcitation to discriminate against background noise. The positions of the individual electron impacts are recorded by a CCD camera and summed over several thousand laser shots to produce the image. Background subtraction is performed by subtraction of a second image for which laser photons are delayed by 1 μs relative to the ion arrival time.

The electric field vector of the detachment laser is polarized parallel to the plane of the imaging detector (along the ion propagation axis). The electric field vector lies along the cylindrical symmetry axis of the photoelectron distribution, and so the full three-dimensional momentum space distribution of photoelectrons can be reconstructed from an image using the BASEX program of Dribinski et al.[13] From the reconstructed momentum space distribution we obtain (by Jacobian transformation) the energy domain photoelectron spectrum and angular distributions.

RESULTS

$I^-{\cdot}(H_2O)_2$. Photoelectron images were recorded over a range of wavelengths for disolvated I^- cluster anions. A typical $I^-{\cdot}(H_2O)_2$ image (247 nm) is shown in Figure 3 (top left), along

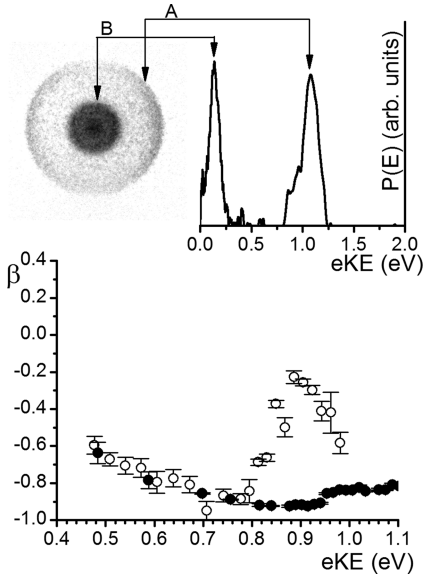

Figure 3. Photodetachment image (top left) and spectrum (top right) at 247 nm. (Bottom) the channel (A) β evolution with eKE for I^- (closed circles)[4] and $I^-{\cdot}(H_2O)_2$ (open circles). Points correspond to different photon energies.

with the accompanying photoelectron spectrum (top right). In the image, higher photoelectron densities are represented as darker areas, and the different direct detachment channels are similar to those of the monosolvated cluster anions yielding either ground ($^2P_{3/2}$) or excited state ($^2P_{1/2}$) iodine atoms.

dx.doi.org/10.1021/jp4104596 | J. Phys. Chem. A 2014, 118, 7249−7254

$$I^-\cdot(H_2O)_2 + h\nu \rightarrow I(^2P_{3/2}) + H_2O + H_2O + e^-$$

(A) [VDE = 3.95 eV]

$$I^-\cdot(H_2O)_2 + h\nu \rightarrow I(^2P_{1/2}) + H_2O + H_2O + e^-$$

(B) [VDE = 4.89 eV]

(VDE = vertical detachment energy). Channel A corresponds to the outer ring in the image. Although the image might at first suggest that channel B possesses greater spectral intensity, the higher photoelectron density observed toward the center of the image is the result of the smaller detector area occupied by photoelectrons associated with this transition. As shown in Figure 3, for 247 nm excitation, the spectral intensities of the two bands are actually rather similar. The two direct detachment bands are separated by the expected 0.94 eV and shifted by 0.91 eV from the energies of the corresponding transitions in I^-, the result of solvation of the atomic iodide anion. Images recorded at wavelengths close to the A threshold show that the degree of neutral H_2O vibrational excitation subsequent to photodetachment is minor and consistent with distortion imparted by the cluster anion environment.

The photoelectron angular distribution maps out the direction of electron ejection with respect to the linearly polarized electric vector of the detachment radiation. For single photon detachment, this is expressed as

$$I(\theta) \propto 1 + \beta\cdot P_2(\cos\theta)$$

where P_2 represents the second Legendre polynomial and β is the previously mentioned anisotropy parameter. For atomic anion detachment, β generally varies gradually with eKE, displaying typical "Cooper−Zare" behavior.[14,15] Figure 3 (bottom) shows the β evolution recorded for the highest eKE $I^-\cdot(H_2O)_2$ transition. Each open circle represents detachment from a different detachment wavelength, and the corresponding value represents an average over the full width at half-maximum of the transition. The filled circles represent detachment from I^- for comparison.[4] The rapid change in the A channel β parameter at photon energies near the channel B threshold (Figure 3) is not consistent with Cooper−Zare direct detachment behavior. Instead the behavior is caused by a dipole-bound-like state (by analogy with previous work on monosolvated cluster anions).[9,16,17] Dipole bound anion states are supported by dipole moments in excess of 2.5 D[18,19] and have been subject to extensive studies by (among others) Jordan and co-workers.[20−28] In the current case, a virtual dipole bound state is associated with an excited I atom within the cluster, $[I(^2P_{1/2})\cdot(H_2O)_2]^-$. This lies in the detachment continuum of $[I(^2P_{3/2})\cdot(H_2O)_2]^-$, and an electronic autodetachment process becomes feasible through I atom relaxation.

$$[I(^2P_{1/2})\cdot(H_2O)_2]^- \rightarrow [I(^2P_{3/2})\cdot(H_2O)_2] + e^-$$
$$\rightarrow I(^2P_{3/2}) + H_2O + H_2O + e^-$$

Autodetachment occurs as the $[I(^2P_{1/2})\cdot(H_2O)_2]^-$ state couples to the channel (A) continuum through energy transfer to the excess electron. The coupling of the ground and excited states of the neutral cluster framework leads to extensive mixing of the angular momentum of the core $[I(^2P_{1/2})\cdot(H_2O)_2]$ and excess electron. It is this angular momentum exchange that leads to the rapid change in the photoelectron angular distributions of electrons in the higher eKE feature of the spectrum. For $I^-\cdot(H_2O)_2$ $\Delta\beta_{max}$ is 0.57.

$I^-\cdot(CH_3CN)_2$. Cluster anion conformers are strongly dependent on ion source conditions. The dashed spectrum in Figure 4a was recorded at a relatively high stagnation pressure of 60 psig (pounds per square inch gauge). In terms of both relative intensity and energies, the two partially resolved transitions (VDE = 3.90 and 4.00 eV) are remarkably similar to previous work, allowing the conclusion that the same conformers are responsible.[2,3] The solid line spectrum in Figure 4a was obtained using a lower stagnation pressure (10 psig), showing that such conditions allow us to selectively produce the conformer with the higher eBE. Subsequent results presented here were obtained at a stagnation pressure of 10 psig.

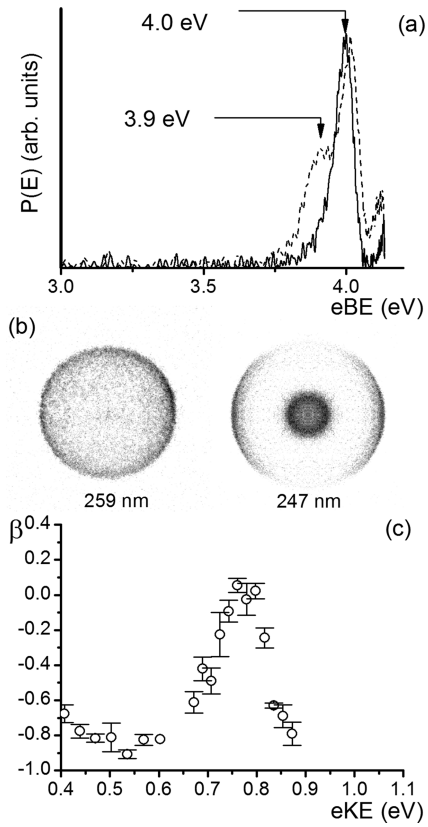

Figure 4. (Top) 300 nm photoelectron spectra of $I^-\cdot(CH_3CN)_2$. Dashed line: high pressure ion source; solid line: low pressure ion source. (Bottom) β vs eKE for the 4 eV transition produced in the low pressure ion source. Each point is due to a different photon energy.

In a manner similar to the $I^-\cdot(H_2O)_2$ results, photoelectron images recorded over a range of wavelengths reveal a rapid change in the angular distribution. This can be clearly seen in the outer ring in the images of Figure 4b recorded at 259 and 247 nm. Plotting β vs eKE (Figure 4c) for this transition clearly shows the result of an autodetachment process analogous to that seen in $I^-\cdot(H_2O)_2$. The maximum in β for the favored low pressure conformer is at 0.79 eV and corresponds to $\Delta\beta_{max}$ = 0.89. This maximum is significantly shifted (in the eKE domain) compared to the 0.91 eV previously reported for $I^-\cdot CH_3CN$.[6]

DISCUSSION

The aim of this paper is to show how the eKE evolution of the PAD can provide crucial experimental information for determining cluster anion geometries. The $I^-\cdot(CH_3CN)_2$

dx.doi.org/10.1021/jp4104596 | J. Phys. Chem. A 2014, 118, 7249−7254

cluster anion, for which conflicting assignments have been previously made[1−3] serves as our demonstration. It is therefore helpful to review the investigations, both experimental and theoretical, that have been made to date.

Previous Experimental Results. Two bands, PES1 (VDE = 3.9 eV) and PES2 (VDE = 4.02 eV) were observed in the 266 nm photoelectron spectrum of $I^-\cdot(CH_3CN)_2$, with PES2 being more intense.[2,3] The transitions were assigned to be of the channel (A) type $[I^-\cdot(CH_3CN)_2 + h\nu \rightarrow I(^2P_{3/2}) + 2CH_3CN + e^-]$ for two different cluster anion conformers. Spectral assignments to the cluster anion conformers I (PES2) and II (PES1) shown in Figure 1 were made on the basis of additive solvent shifts.[3] PES2 is shifted from free I^- detachment by twice the amount observed for $I^-\cdot CH_3CN$, suggesting similar proximity of both acetonitrile molecules to the anion.

The photoneutral action spectrum (3.7−4.2 eV) in the region of the channel A threshold also contained two bands (PNS1 and PNS2).[2,3] The more intense photoneutral band (PNS1) maximum was found at photon energy 3.86 eV, 40 meV below the VDE of the lower intensity photoelectron spectral band (PES1) and 150 meV below the PES2 VDE. Photoexcitation in the PNS1 region produced monomer CH_3CN^- and dimer $(CH_3CN)_2^-$ dipole bound anions. Excitation in the vicinity of the PNS2 band produced no anionic photoproducts.[2,3,29]

These observations lead to association of the more intense PNS1 band with cluster anion conformer II. It was argued that the conformer II arrangement allows excitation to a head-to-tail $[I\cdot CH_3CN\cdot CH_3CN]^-$ dipole-bound anion. This would greatly enhance the photoabsorption cross section and account for the intensity difference between the PES1 and PNS1 bands. The observed product dimer dipole bound anion would then have a $[CH_3CN\cdot CH_3CN]^-$ head-to-tail arrangement produced by loss of the iodine atom due to rearrangement subsequent to photoexcitation.[30]

Previous Calculations. These assignments are challenged by ab initio calculations for parent cluster and dipole bound acetonitrile anions.[1,31] Cluster anion geometry optimization predicted the existence of a third cluster anion conformer as shown in Figure 1.[1] Calculation indicated that cluster anion conformers I and III have similar stabilities, while conformer II was predicted to be 3−4 kcal mol^{-1} less stable.[1]

Time-dependent density functional theory predicted vertical excitation energies (VEEs) to charge transfer to solvent states (near the $I(^2P_{3/2}) + 2CH_3CN + e^-$ direct detachment threshold) for each conformer of 3.7 eV (III), 3.6 eV (I) and 2.8 eV (II).[1] Although the calculations significantly underestimate the experimentally recorded values,[3] they do suggest that the excitation energies for conformers I and III are close to one another while the conformer II VEE is likely to be significantly lower. As a result of these calculations, a change in the assignment of the photoelectron spectral transitions was suggested.[1] The PES1 transition was reassigned to conformer I and the PES2 transition to the hydrogen bonded conformer. The absence of the much lower binding energy conformer was presumed to be the result of unfavorable source conditions for the formation of conformer II.

Current Work in the Context of Previous Studies. Figure 5 (solid circles) shows the $\Delta\beta_{max}$ values obtained for various monosolvated I^- cluster anions. As has been previously demonstrated, there is a near linear correlation between the dipole moment of the atomic framework of monosolvated cluster anions and $\Delta\beta_{max}$ for channel (A) electrons.[6]

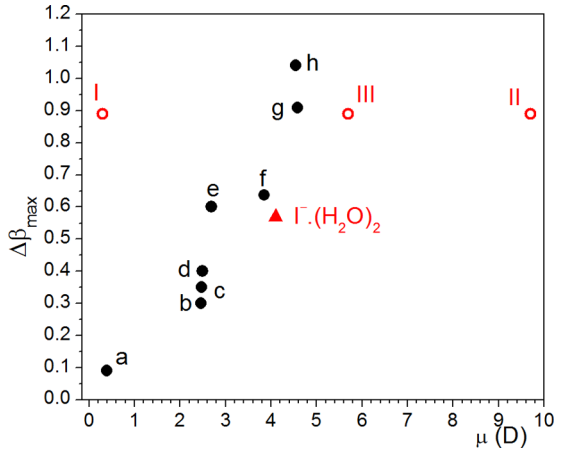

Figure 5. Comparison of $\Delta\beta_{max}$ with calculated μ for neutral cluster frameworks. Solid circles represent $I^-\cdot X$ with X = (a) CO_2, (b) H_2O, (c) CH_3Cl, (d) CH_3Br, (e) pyrrole, (f) acetone, (g) nitromethane, or (h) acetonitrile. The solid triangle represents $I^-\cdot(H_2O)_2$, and the open circles represent the three $I^-\cdot(CH_3CN)_2$ conformers (see Figure 1).

Comparison of dihydrated I^- cluster anion detachment to these monosolvated results (Figure 5 closed triangle) shows very good agreement with the trend, strongly suggesting that the correlation is preserved in disolvated cluster anions. The dipole moment for the $I\cdot(H_2O)_2$ cluster framework (in the limit of vertical excitation)[7] was calculated via Gaussian 03[32] at the MP2 level and the aug-cc-pvdz basis set[33] for all atoms except I, for which we used the CRENBL pseudopotential and basis set.[33−35]

The dipole moments of the neutral daughters of the three conformers of $I^-\cdot(CH_3CN)_2$ (at the cluster anion minima) were calculated in a similar manner. These are found to be μ_I = 0.3 D, μ_{II} = 9.7 D and μ_{III} = 5.7 D. Plotting the observed $\Delta\beta_{max}$ value (0.89) for each of these dipole moments in Figure 5 (open circles) clearly shows that only conformer III is consistent with the monosolvated trend.

The rapid change we observe in the channel A β parameter below the channel B threshold is the result of excitation to a temporary excited state of the cluster framework $[I(^2P_{1/2})\cdot(CH_3CN)_2]^-$ and subsequent I atom relaxation.[6] It is no coincidence that the maximum in β(eKE) is 150 meV below the channel B threshold, the same difference as that between the PNS1 and PES2 maxima for channel A. The excited $[I(^2P_{1/2})\cdot(CH_3CN)_2]^-$ state can be thought of as analogous to the one responsible for the PNS1 band, which is a dipole bound state associated with the ground state $[I(^2P_{3/2})\cdot(CH_3CN)_2]$ framework .[2,3] Where the previous calculations and experimental work differ is in the nature of the conformer, which supports this state. The present results are consistent with the interpretation of the theoretical study in which conformer III supports the initial dipole bound state.

The question remains as to whether this interpretation is consistent with the formation of the observed asymptotic product dipole bound anions. It was previously established that excitation in the region of the PNS1 transition (3.85 eV) produces acetonitrile dimer (and monomer) anions while excitation in the region of PNS2 does not.[3] Thus 3.85 eV photoexcitation results in a physically bound state that ultimately evolves to acetonitrile dimer and monomer anions via loss of the I atom.

dx.doi.org/10.1021/jp4104596 | J. Phys. Chem. A 2014, 118, 7249−7254

Calculation has shown that there are two local minima on the acetonitrile dimer anion ground state potential energy surface.[31,36] These are shown in Figure 6 and represent a head-to-tail dipole bound anion (VDE = 102 meV) (a) and a symmetric, solvated electron type structure (VDE = 155 meV) (b).[36] A head-to-tail parent cluster anion (Figure 1, II) might reasonably be expected to produce a head-to-tail dipole bound dimer (Figure 6a) with relatively low levels of van der Waals excitation. However, conformer II is inconsistent with both the observed anisotropy data and ab initio calculation of detachment energies. The symmetric cluster anion (Figure 1, I) has the two acetonitriles arranged in the correct manner. However, trajectory calculations from this geometry suggest that the photo excited cluster will form monomer rather than dimer anions.[30] Additionally, the assignment to a symmetric parent cluster anion is again inconsistent with prior calculation and our anisotropy data.

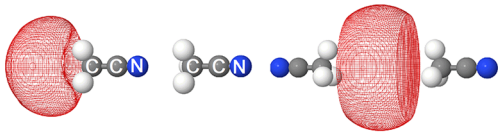

Figure 6. Physically bound dimer anion orbitals for geometries optimized at the MP2 level of theory.[36] (a) Head-to-tail dipole bound anion. (b) Acetonitrile solvated electron.

Our photoelectron anisotropy data is most consistent with excitation from the hydrogen bonded cluster anion (Figure 1, III). This would constrain the two acetonitrile molecules to lie with their C_3 axes at angles intermediate to the head-to-tail or acetonitrile solvated electron extremes. Examination of the dimer anion potential energy surface[36] allows us to conjecture that dimer anions are likely to undergo wide amplitude motions, but that trapping of the dimer anions on this surface (rather than complete fragmentation) is at least feasible when photoexciting from the hydrogen bonded cluster anion.[2,3,37] We note that this interpretation is at least consistent with the observed $\Delta\beta_{max}$ value (hydrogen bonded cluster anion structure) and observed 150 meV energy difference in the detachment and absorption spectra. We are currently performing a pump−probe photodetachment study to further investigate the nature of the dimer anions produced.

SUMMARY

Photoelectron imaging measurements of the disolvated $I^-\cdot(H_2O)_2$ and $I^-\cdot(CH_3CN)_2$ cluster anions were performed over a range of photon energies. The channel A photoelectron angular distributions undergo a sharp change in both cases at photodetachment near the channel B threshold. This effect is also seen in monosolvated I^- cluster anions where $\Delta\beta_{max}$ has been observed to correlate well with the dipole moment of the neutral cluster framework. Results for $I^-\cdot(H_2O)_2$ indicate that the correlation is preserved in multiply solvated anions. Through tuning of the ion source conditions, a single $I^-\cdot(CH_3CN)_2$ conformer is produced for which $\Delta\beta_{max}$ is consistent with a cluster framework dipole moment of 5.7 D, which supports assignment of the 4.0 eV transition in the photoelectron spectrum to a hydrogen bonded conformer.

Of course, it still remains to obtain a full understanding of the relationship between the cluster framework dipole moment and $\Delta\beta_{max}$. In this regard, parallels with treatments of processes involving relaxation via electron-loss in excited neutral atomic, molecular and cluster species such as Rydberg state autoionization,[38] interatomic Coulombic decay[39] and electron transfer mediated decay will be instructive.[40,41] Nevertheless, the data presented here demonstrate the intriguing possibility that the eKE evolution of the PAD might be used for structural analysis of small cluster anions.

AUTHOR INFORMATION

Corresponding Authors

*Fax: +267 355 2836; Tel: +267 355 2485; E-mail: fmbaiwa@gmail.com.

*Fax: +1 314 935 4481; Tel: +1 314 935 5928; E-mail: mabbs@wustl.edu

Notes

The authors declare no competing financial interest.

ACKNOWLEDGMENTS

The authors gratefully acknowledge support by the National Science Foundation (Grant CHE-0748738).

REFERENCES

(1) Timerghazin, Q. K.; Nguyen, T. N.; Peslherbe, G. H. *J. Chem. Phys.* **2002**, *116*, 6867−6870.
(2) Dessent, C. E. H.; Bailey, C. G.; Johnson, M. A. *J. Chem. Phys.* **1995**, *103*, 2006−2015.
(3) Dessent, C. E. H.; Kim, J.; Johnson, M. A. *Acc. Chem. Res.* **1998**, *31*, 527−534.
(4) Mbaiwa, F.; Wei, J.; Van Duzor, M.; Mabbs, R. *J. Chem. Phys.* **2010**, *132*, 134304.
(5) Van Duzor, M.; Wei, J.; Mbaiwa, F.; Mabbs, R. *J. Chem. Phys.* **2010**, *133*, 144303.
(6) Mbaiwa, F.; Dao, D.; Holtgrewe, N.; Lasinski, J.; Mabbs, R. *J. Chem. Phys.* **2012**, *136*, 114303.
(7) Lee, H. M.; Kim, K. S. *J. Chem. Phys.* **2001**, *114*, 4461−4471.
(8) Van Duzor, M.; Mbaiwa, F.; Wei, J.; Mabbs, R. *J. Chem. Phys.* **2009**, *131*, 204306.
(9) Mbaiwa, F.; Van Duzor, M.; Wei, J.; Mabbs, R. *J. Phys. Chem. A* **2010**, *114*, 1539−1547.
(10) Osborn, D. L.; Leahy, D. J.; Cyr, D. M.; Neumark, D. M. *J. Chem. Phys.* **1996**, *104*, 5026−5039.
(11) Wiley, W. C.; McLaren, I. H. *Rev. Sci. Instrum.* **1955**, *26*, 1150−1157.
(12) Eppink, A. T. J. B.; Parker, D. H. *Rev. Sci. Instrum.* **1997**, *68*, 3477−3484.
(13) Dribinski, V.; Ossadtchi, A.; Mandelshtam, V. A.; Reisler, H. *Rev. Sci. Instrum.* **2002**, *73*, 2634−2642.
(14) Cooper, J.; Zare, R. N. *J. Chem. Phys.* **1968**, *48*, 942−943.
(15) Cooper, J.; Zare, R. N. *J. Chem. Phys.* **1968**, *49*, 4252.
(16) Bowen, M. S.; Beccucci, M.; Continetti, R. E. *J. Phys. Chem. A* **2005**, *109*, 11781−11792.
(17) Bowen, M. S.; Beccucci, M.; Continetti, R. E. *J. Chem. Phys.* **2006**, *125*, 133309.
(18) Crawford, O. H. *Mol. Phys.* **1971**, *20*, 585−591.
(19) Crawford, O. H.; Garrett, W. R. *J. Chem. Phys.* **1977**, *66*, 4968−4970.
(20) Jordan, K. D. *Acc. Chem. Res.* **1979**, *12*, 36−42.
(21) Jordan, K. D.; Wang, F. *Annu. Rev. Phys. Chem.* **2003**, *54*, 367−396.
(22) Jordan, K. D.; Wendoloski, J. J. *Chem. Phys.* **1977**, *21*, 145−154.
(23) Gutowski, M.; Skurski, P.; Boldyrev, A. I.; Simons, J.; Jordan, K. D. *Phys. Rev. A* **1996**, *54*, 1906−1909.
(24) Gutowski, M.; Skurski, P.; Jordan, K. D.; Simons, J. *Int. J. Quantum Chem.* **1997**, *64*, 183−191.

(25) Gutowski, M.; Jordan, K. D.; Skurski, P. *J. Phys. Chem. A* **1998**, *102*, 2624−2633.
(26) Vila, F. D.; Jordan, K. D. *J. Phys. Chem. A* **2002**, *160*, 1391−1397.
(27) Hammer, N. I.; Diri, K.; Jordan, K. D.; Desfrancois, C.; Compton, R. N. *J. Chem. Phys.* **2003**, *119*, 3650−3660.
(28) Sommerfeld, T.; Jordan, K. D. *J. Am. Chem. Soc.* **2006**, *128*, 5828−5833.
(29) Dessent, C. E. H.; Kim, J.; Johnson, M. A. *J. Phys. Chem.* **1996**, *100*, 12−14.
(30) Takayanagi, T. *J. Phys. Chem. A* **2006**, *110*, 7011−7018.
(31) Timerghazin, Q. K.; Peslherbe, G. H. *J. Phys. Chem. B* **2008**, *122*, 520−528.
(32) Frisch, M. J.; Trucks, G. W.; Schlegel, H. B.; Scuseria, G. E.; Robb, M. A.; Cheeseman, J. R.; Montgomery, J. A., Jr.; Vreven, T.; Kudin, K. N.; Burant, J. C.; Millam, J. M.; Iyengar, S. S.; Tomasi, J.; Barone, V.; Mennucci, B.; Cossi, M.; Scalmani, G.; Rega, N.; Petersson, G. A.; Nakatsuji, H.; Hada, M.; Ehara, M.; Toyota, K.; Fukuda, R.; Hasegawa, J.; Ishida, M.; Nakajima, T.; Honda, Y.; Kitao, O.; Nakai, H.; Klene, M.; Li, X.; Knox, J. E.; Hratchian, H. P.; Cross, J. B.; Bakken, V.; Adamo, C.; Jaramillo, J.; Gomperts, R.; Stratmann, R. E.; Yazyev, O.; Austin, A. J.; Cammi, R.; Pomelli, C.; Ochterski, J. W.; Ayala, P. Y.; Morokuma, K.; Voth, G. A.; Salvador, P.; Dannenberg, J. J.; Zakrzewski, V. G.; Dapprich, S.; Daniels, A. D.; Strain, M. C.; Farkas, O.; Malick, D. K.; Rabuck, A. D.; Raghavachari, K.; Foresman, J. B.; Ortiz, J. V.; Cui, Q.; Baboul, A. G.; Clifford, S.; Cioslowski, J.; Stefanov, B. B.; Liu, G.; Liashenko, A.; Piskorz, P.; Komaromi, I.; Martin, R. L.; Fox, D. J.; Keith, T.; Al-Laham, M. A.; Peng, C. Y.; Nanayakkara, A.; Challacombe, M.; Gill, P. M. W.; Johnson, B.; Chen, W.; Wong, M. W.; Gonzalez, C.; Pople, J. A. *Gaussian 03*, Revision C.02, Gaussian, Inc.: Wallingford, CT, 2004.
(33) Dunning, T. H. *J. Chem. Phys.* **1989**, *90*, 1007−1023.
(34) LaJohn, L. A.; Christiansen, P. A.; Ross, R. B.; Atashroo, T.; Ermler, W. C. *J. Chem. Phys.* **1987**, *87*, 2812−2824.
(35) Combariza, J. E.; Kestnet, N. R.; Jortner, J. *J. Chem. Phys.* **1994**, *100*, 2851−2864.
(36) Takayanagi, T. *J. Chem. Phys.* **2005**, *122*, 244307.
(37) Dessent, C. E. H.; Kim, J.; Johnson, M. A. *J. Phys. Chem.* **1996**, *100*, 12−14.
(38) Johnson, W. R.; Cheng, K. T.; Huang, K.-M.; Le Dourneuf, M. *Phys. Rev. A* **1980**, *22*, 989−997.
(39) Cederbaum, L. S.; Zobeley, J.; Tarantelli, F. *Phys. Rev. Lett.* **1997**, *79*, 4778−4781.
(40) Zobeley, J.; Santra, R.; Cederbaum, L. S. *J. Chem. Phys.* **2001**, *115*, 5076−5088.
(41) Averbukh, V.; Cederbaum, L. S. *J. Chem. Phys.* **2005**, *123*, 204107.